PNAS RESEARCH ARTICLE | BIOCHEMISTRY

Endocannabinoid biosynthetic enzymes regulate pain response via LKB1–AMPK signaling

Miaomiao Chen[a,1], Myungsun Shin[a,1], Timothy B. Ware[a,1], Giulia Donvito[b], Karan H. Muchhala[b], Ryan Mischel[b], Mohammed A. Mustafa[b], Vlad Serbulea[c], Clint M. Upchurch[c], Norbert Leitinger[c], Hamid I. Akbarali[b], Aron H. Lichtman[b,d], and Ku-Lung Hsu[a,c,e,f,2,3]

Edited by Benjamin Cravatt, The Scripps Research Institute, La Jolla, CA; received March 24, 2023; accepted November 8, 2023

Diacylglycerol lipase-beta (DAGLβ) serves as a principal 2-arachidonoylglycerol (2-AG) biosynthetic enzyme regulating endocannabinoid and eicosanoid metabolism in immune cells including macrophages and dendritic cells. Genetic or pharmacological inactivation of DAGLβ ameliorates inflammation and hyper-nociception in preclinical models of pathogenic pain. These beneficial effects have been assigned principally to reductions in downstream proinflammatory lipid signaling, leaving alternative mechanisms of regulation largely underexplored. Here, we apply quantitative chemical- and phospho-proteomics to find that disruption of DAGLβ in primary macrophages leads to LKB1–AMPK signaling activation, resulting in reprogramming of the phosphoproteome and bioenergetics. Notably, AMPK inhibition reversed the antinociceptive effects of DAGLβ blockade, thereby directly supporting DAGLβ–AMPK crosstalk in vivo. Our findings uncover signaling between endocannabinoid biosynthetic enzymes and ancient energy-sensing kinases to mediate cell biological and pain responses.

endocannabinoids | diacylglycerol lipase | activity based protein profiling | AMPK | inflammation

Significance

Here, we identified diacylglycerol lipase-beta (DAGLβ) as a principal regulator of AMP-activated protein kinase (AMPK) activation in primary macrophages and in vivo. DAGLβ disruption enhanced membrane liver kinase B1 (LKB1) activity and subsequent AMPK activation to regulate the bioenergetic state of macrophages. Notably, AMPK inhibition reversed the antinociceptive phenotype of *Daglb* deficient mice, which could be explained in part by effects on hyper-excitability of dorsal root ganglion neurons. Our findings provide important mechanistic insights into crosstalk between endocannabinoid biosynthesis and bioenergetic regulation and support disruption of DAGLβ as a targeted approach for activating AMPK signaling to block inflammation and related pain.

Diacylglycerol lipase-beta (DAGLβ) and the functionally related DAGLα isoform represent key biosynthetic enzymes of the endocannabinoid, 2-arachidonoylglycerol (2-AG) and downstream metabolic product arachidonic acid (AA) (1–3). These transmembrane serine hydrolases regulate cell signaling by hydrolyzing diacylglycerol (DAG) lipid messengers including the 2-AG precursor and PKC agonist SAG (4, 5). DAGLα functions principally in central tissues (2, 3, 6–11) (e.g., brain and spinal cord) while DAGLβ activity is enriched in liver (2) and immune cells including macrophages (12), microglia (13), and dendritic cells (14). DAGLβ inactivation affects peripheral prostaglandins and inhibitors of this serine hydrolase have been likened to nonsteroidal antiinflammatory drugs (NSAIDs) in preclinical pain models, but without ulcerogenic effects (15). The prominent effects of DAGLβ inhibitors in neuropathic pain, however, suggest pharmacological mechanisms beyond AA-prostaglandin signaling alone (16, 17).

Emerging studies on the role of exercise and caloric restriction in pain modulation identified an intriguing connection between bioenergetics and endocannabinoids (18, 19). Regulation of energy homeostasis is mediated principally through sensing of low cellular ATP levels through an evolutionarily conserved system mediated by AMP-activated protein kinase (AMPK) (20, 21). AMPK can monitor energy availability and respond to changes in the ATP/ADP and ATP/AMP ratio through direct binding of adenine nucleotides (22, 23) and activation of its kinase activity (23–26). Once activated, AMPK reprograms cellular metabolism through regulation of the phosphoproteome toward decreased anabolism and increased catabolism (20, 21). Pharmacological activation of AMPK can produce therapeutic responses in the clinic. The antihyperglycemic drug metformin activates AMPK to regulate glucose metabolism for treatment of type 2 diabetes (27). The NSAID aspirin also acts as an AMPK activator to induce a pseudo-starved state of macrophages that suppresses inflammation (28). Depending on the biological system, activation of the endocannabinoid system can stimulate (29–31) or inhibit AMPK (32). These disparate findings underscore the need for additional studies aimed at understanding AMPK-endocannabinoid crosstalk and regulation in the context of pain signaling.

AMPK is a heterotrimeric complex that consists of a single α- (catalytic), β- (regulatory), and γ- (regulatory) subunit (20, 21). In humans, multiple isoforms of each subunit are encoded by different genes: α-subunit (*PRKAA1* and *PRKAA2*), β-subunit (*PRKAB1* and *PRKAB2*), and γ-subunit (*PRKAG1*, *PRKAG2*, and *PRKAG3*). The γ-subunit binds AMP (and ADP to a lesser extent) to stimulate AMPK activity through a key phosphorylation on threonine 172 (T172) in the α-subunit that contains the kinase domain (22–26). The β-subunit allows AMPK to bind and respond to glycogen (33). AMPK T172 phosphorylation is mediated by the upstream kinases liver kinase B1 (24, 34) (LKB1, encoded by *STK11*) and calcium/calmodulin-dependent protein kinase 2 (35, 36) (CAMKK2).

Author contributions: N.L., H.I.A., A.H.L., and K.-L.H. designed research; M.C., M.S., T.B.W., G.D., K.H.M., R.M., M.A.M., V.S., and C.M.U. performed research; M.C., M.S., T.B.W., G.D., K.H.M., R.M., M.A.M., V.S., C.M.U., N.L., H.I.A., A.H.L., and K.-L.H. analyzed data; K.-L.H. supervision of the project; and M.C., M.S., T.B.W., and K.-L.H. wrote the paper.

The authors declare no competing interest.

This article is a PNAS Direct Submission.

[1]M.C., M.S., and T.B.W. contributed equally to this work.

[2]To whom correspondence may be addressed. Email: ken.hsu@austin.utexas.edu.

[3]Present address: Department of Chemistry, University of Texas at Austin, Austin, TX 78712.

This article contains supporting information online at https://www.pnas.org/lookup/suppl/doi:10.1073/pnas.2304900120/-/DCSupplemental.

Published December 18, 2023.

Mutations in *STK11* cause the autosomal dominant disorder Peutz-Jeghers syndrome and these patients are at high risk for developing tumors (37). Biochemical and genetic analyses demonstrate that LKB1 mediates the bulk of AMPK activation in response to conditions of energy stress (38). The upstream regulatory mechanisms of LKB1 are poorly defined although recent studies have identified lipids as potential mediators (39).

Here, we identified DAGLβ as a principal regulator of LKB1–AMPK activation in primary macrophages and in vivo. We discovered crosstalk between endocannabinoid biosynthetic and AMPK pathways in primary macrophages using chemoproteomic and phosphoproteomic profiling. DAGLβ disruption enhanced membrane LKB1 activity and subsequent AMPK activation to regulate the bioenergetic state of macrophages. Notably, AMPK inhibition reverses the antinociceptive phenotype of DAGLβ KO mice, which could be explained in part by effects on hyperexcitability of dorsal root ganglion neurons. Collectively, our findings describe blockade of endocannabinoid biosynthesis as a targeted AMPK activation mechanism in vivo.

Results

Kinome Profiling Reveals Enhanced LKB1 Activity in DAGLβ-Disrupted Macrophages. Genetic or pharmacological disruption of DAGLβ alters cellular levels of key signaling lipids including diacylglycerol (DAG), endocannabinoid (2-AG), and eicosanoid lipids (1, 2, 12). Each of these lipids can signal through cognate receptor proteins to position DAGLβ as a potential metabolic "hub" for regulating diverse cell biology (Fig. 1). While these prior studies focused on assigning DAGLβ as a key 2-AG biosynthetic enzyme, global analyses can reveal unanticipated regulatory mechanisms mediated by DAGLβ in cell biology. We selected primary macrophages as our model system because of the enriched activity and importance of DAGLβ in regulating innate immune responses (12–14).

We reasoned that a global assessment of changes in kinase functional profiles in DAGLβ-disrupted systems may reveal crosstalk between lipid and protein signaling to further illuminate the cell biological functions of this key endocannabinoid biosynthetic enzyme. These functional proteomic studies are especially important given that our transcriptomic analyses did not reveal overt changes in gene expression upon genetic disruption of DAGLβ in primary macrophages (*SI Appendix*, Fig. S1). To enable quantitative proteomics, we differentiated bone marrow-derived macrophages (BMDMs) in SILAC media to generate "light" and "heavy" BMDMs for our tandem liquid chromatography-mass spectrometry (LC-MS/MS) studies as previously reported (40). We performed lipopolysaccharide (LPS, 100 ng/mL, 16 h) stimulations to confirm that SILAC light and heavy BMDMs showed comparable inflammatory responses as determined by elevated TNFα secretion. Genetic knockout (KO) of DAGLβ resulted in significantly reduced LPS-stimulated TNFα release from BMDMs, which matched previous reports in macrophages (12, 13) (*SI Appendix*, Fig. S2).

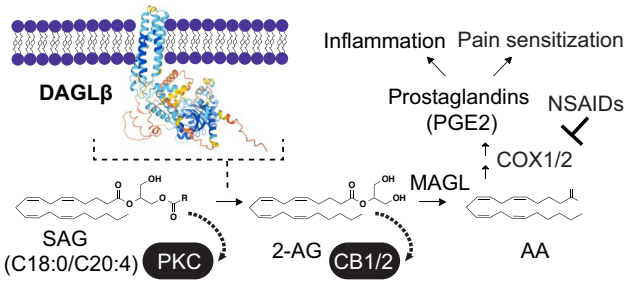

Fig. 1. DAGLβ regulation of lipid signaling. DAGLβ biosynthesizes 2-arachidonylglycerol (2-AG) through *sn*-1 specific hydrolysis of arachidonic acid-esterified diacylglycerols (1-stearoyl-2-arachidonoylglycerol or SAG shown as a principal substrate). Blockade of DAGLβ results in DAG accumulation and 2-AG reduction that can affect protein kinase C and endocannabinoid receptor (CB1 and CB2) signaling, respectively. The 2-AG pool regulated by DAGLβ can be further hydrolyzed by 2-AG hydrolases (monoacylglycerol lipase or MAGL as an example) to produce arachidonic acid (AA) utilized by COX enzymes for biosynthesizing prostaglandins (PGE2). Akin to nonsteroidal antiinflammatory drugs (NSAIDs), DAGLβ inhibitors reduce inflammation through blockade of prostaglandin signaling. The AlphaFold structure of DAGLβ is shown (AF-Q91WC9-F1).

We utilized ATP acyl phosphate activity-based protein profiling (ABPP) to gain insights into signaling alterations in DAGLβ-disrupted BMDMs (*SI Appendix*, Fig. S3*A*). This class of activity-based probe facilitates covalent modification of conserved lysines in the ATP-binding pocket for assessing activity states of protein and lipid kinases (41–43) (*SI Appendix*, Fig. S3*B*). SILAC light and heavy BMDMs derived from DAGLβ wild-type (WT) and KO mice, respectively, were lysed, fractionated into soluble and membrane proteomes, and treated with ATP acyl phosphates to label active-site lysines. Light and heavy proteomes were combined after probe labeling followed by digestion with trypsin protease, enrichment of desthiobiotin-modified peptides by avidin-affinity chromatography, and LC-MS/MS analysis to quantify isotopically tagged active-site peptides of kinases. See *SI Appendix* for additional details of the LC-MS ABPP procedure including the quality control confidence criteria for evaluation of probe-modified peptides.

Using this approach, we quantified changes in probe binding on 170 kinases (>260 distinct modified K sites) in DAGLβ WT compared with KO BMDMs under basal and LPS-activated states (Fig. 2 *A*–*C* and *SI Appendix*, Fig. S4). The majority of probe-modified sites quantified did not show substantial changes with DAGLβ disruption (median SILAC heavy (KO)/light (WT) ratio or SR ~0.7, Dataset S1). Strikingly, we observed a >10-fold enhancement in probe binding to membrane LKB1 (encoded by *Stk11*) in DAGLβ KO compared with WT LPS-stimulated BMDMs (K178 site, SR >20; Fig. 2*D*). The K178 site is conserved between mouse and human LKB1 and located adjacent to the HxD motif of the catalytic loop (44–46). The probe-modified peptide containing the K178 site matches the consensus sequence targeted by ATP acyl phosphates (42, 43). In contrast, probe binding to LKB1 in the soluble fraction LPS counterpart and total LKB1 protein expression was largely unchanged, which supports functional probe binding changes in contrast with general alterations in protein expression (SR = 0.9, Fig. 2 *D* and *E* and *SI Appendix*, Fig. S5).

DAGLβ Disruption Activates AMPK in Primary Macrophages. The prominent increase in ATP acyl phosphate probe labeling of LKB1 K178 in membrane fractions of DAGLβ-deficient BMDMs suggested potential crosstalk between endocannabinoid biosynthetic and LKB1–AMPK pathways. Previous studies demonstrated that membrane localization of LKB1 is needed for AMPK activation in mammalian cells (39, 47) and mutagenesis of the HxD motif adjacent to K178 resulted in impaired LKB1 phosphorylation of AMPK (46). We compared the levels of phospho-AMPK (T172) in DAGLβ KO and WT BMDMs in the absence and presence of LPS stimulation. DAGLβ expression and activity were assessed using western blots and the DAGL-directed activity-based probe (HT-01) (12), respectively. Total AMPK levels were largely consistent across the treatment conditions. In contrast, phospho-AMPK (pAMPK) levels were significantly increased in LPS-stimulated DAGLβ KO compared

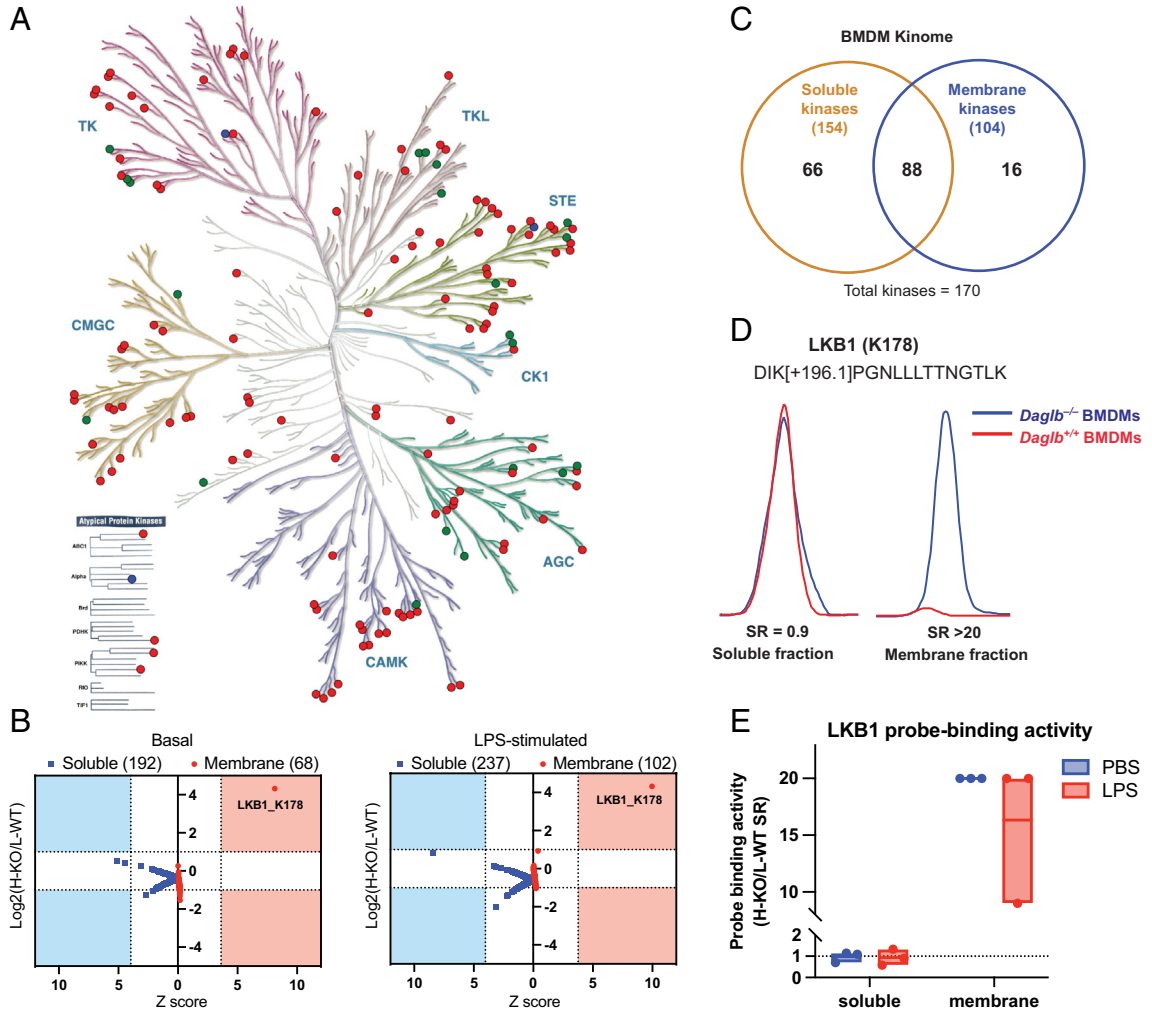

Fig. 2. LKB1 ATP-probe binding activity is enhanced in DAGLβ-disrupted BMDMs. (*A*) Kinome tree of ATP acyl phosphate probe binding activity to kinase active sites (142 protein kinases, 28 metabolic kinases) detected by quantitative chemical proteomics under basal (blue circles, 3 kinases), LPS-stimulated (green circles, 21 kinases), and both treatment conditions (red circles, 118 kinases). Lysates from DAGLβ WT and KO BMDMs (basal and LPS activated) were fractionated to soluble and membrane proteomes for kinome profiling studies. The SILAC ratio (SR) was determined by heavy (KO)/light (WT) peptide area under the curve of MS1 extracted ion chromatograms (EICs). Kinome tree illustration reproduced courtesy of Cell Signaling Technology, Inc. (http://www.cellsignal.com). (*B*) The SR values [$\log_2$(H-KO/L-WT)] were plotted as a function of the Z score to identify statistically significantly increased (*Top* quadrants) or decreased (*Bottom* quadrants) probe binding to kinases detected in soluble (blue shading) and membrane fractions (red shading; >twofold change, $P < 0.01$). (*C*) ATP acyl phosphates broadly profile probe binding activity of the BMDM kinome. (*D*) Representative MS1 EICs of STK11 (LKB1) probe-modified (K178) peptide show a striking enhancement in binding activity in membrane but not soluble fractions of DAGLβ KO (heavy, blue) versus WT (light, red) BMDM proteomes under basal and LPS-activated states. (*E*) Quantitation of LKB1 K178 probe-modified peptide across BMDMs derived from independent littermate pairs of DAGLβ WT and KO mice. Data are shown as mean ± SEM and representative of n = 3 biologically independent replicates. See Dataset S1 for complete list of SR values for kinase binding sites quantified.

with WT BMDMs and treatment with the AMPK inhibitor dorsomorphin (48) (10 μM, 4 h) reduced pAMPK levels (Fig. 3*A* and *SI Appendix*, Fig. S6). Dorsomorphin can reduce pAMPK levels by altering conformation of the activation loop (containing T172) upon binding to reduce phosphorylation by AMPK kinases and/or promote dephosphorylation of T172 by phosphatases (49).

Next, we tested whether this AMPK signaling effect could be recapitulated with acute perturbation using the DAGLβ-selective inhibitor KT109 (12). We treated WT BMDMs from C57BL/6 J mice (naive or LPS-stimulated) with KT109 (200 nM, 4 h) followed by HT-01-based ABPP confirmation of DAGLβ inactivation and western blot evaluation of AMPK activation. We observed substantial DAGLβ inhibition from KT109 treatments in BMDMs under basal and LPS-activated conditions (~70 to 90%, Fig. 3*B*). Total AMPK expression levels in BMDMs appeared to be elevated with LPS stimulation. In agreement with our genetic disruption data, pAMPK levels in BMDMs were significantly enhanced with KT109 treatments, and dorsomorphin reversed this activation event (Fig. 3*B* and *SI Appendix*, Fig. S6).

To assess the functional impact of DAGLβ–AMPK crosstalk, we first performed LC-MS/MS proteomics to assess global alterations in DAGLβ KO (SILAC heavy) compared with WT (SILAC light) BMDM proteomes. Gene Ontology (GO) analysis revealed enrichment for biological processes related to energy metabolism (ATP synthesis, oxidative phosphorylation, and ATP synthesis coupled electron transport) as well as general catabolic processes (*SI Appendix*, Fig. S7). These proteomic findings are supportive of AMPK activation that is characterized by a shift in metabolism from anabolic (e.g., fatty acid production, protein biosynthesis) to catabolic processes (e.g., glycolysis, fatty acid oxidation) (20, 21). As a result, cells exhibit more aerobic and glycolytic characteristics that collectively present as an enhanced bioenergetic phenotype.

We measured the cellular bioenergetic profiles of BMDMs using extracellular flux assays to directly assess ex vivo the extracellular

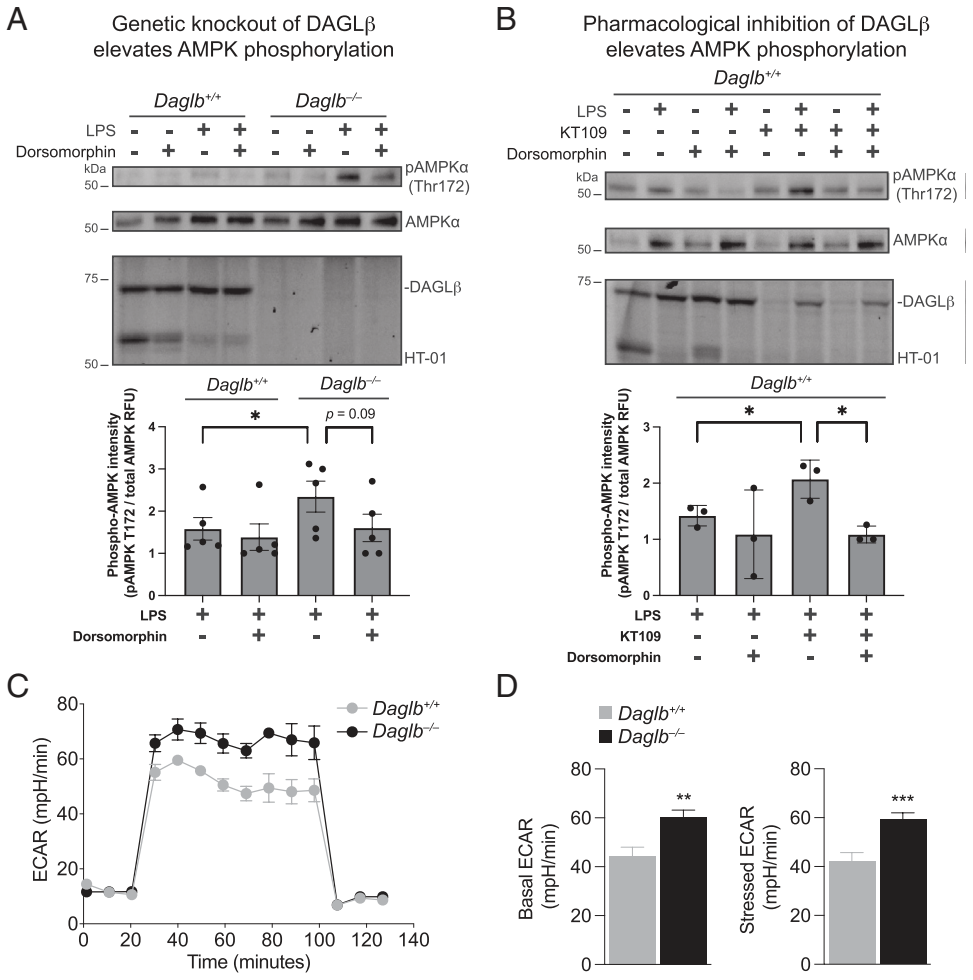

Fig. 3. AMPK activation in DAGLβ-disrupted BMDMs. (*A*) Live-cell treatment of AMPK inhibitor dorsomorphin (10 μM, 4 h) in DAGLβ KO and WT cells. Compound treatment was performed after LPS stimulation (100 ng/mL, 16 h). Antibodies were used for detecting AMPK and phospho-AMPK (Thr172) protein levels by western blot. The serine hydrolase probe HT-01 (1 μM, 30 min at 37 °C) was used for ABPP analysis of DAGLβ. Bar plot of the quantified pAMPK/AMPK protein signals (RFU, LPS stimulated conditions) as determined by western blot. Data shown are mean ± SEM. A two-sample Student's *t* test was used to evaluate statistical significance. $*P < 0.05$. (n = 5 biologically independent replicates). (*B*) BMDMs were stimulated with LPS (100 ng/mL, 16 h), followed by in situ treatment with KT109 (200 nM, 4 h) and/or dorsomorphin (10 μM, 4 h). BMDM membrane proteomes from treated cells were used for HT-01 analysis (1 μM, 30 min at 37 °C). BMDM-soluble proteomes were used for western blot analysis and quantification of AMPK and phospho-AMPK (Thr172) levels. Data shown are mean ± SEM. Statistical significance was determined using a two-sample Student's *t* test. $*P < 0.05$. (n = 3 biologically independent replicates). (*C* and *D*) Analysis of cellular bioenergetics by a glycolytic stress test. DAGLβ WT and DAGLβ KO BMDMs were analyzed using a Seahorse XF analyzer to interrogate basal and stressed extracellular acidification rates (ECAR) of cells. See *SI Appendix*, *Materials and Methods* for additional details. Statistical significance was determined by a Welch's two-sided *t* test; $*P < 0.05$, $**P < 0.01$, $***P < 0.001$. All data shown represent mean ± SEM; (n = 23 to 25 samples). All data shown are representative of n = 5 biologically independent experiments.

acidification rate (ECAR, measure of aerobic glycolysis) and oxygen consumption rate (OCR, measure of oxidative phosphorylation) (50). We measured the glycolytic capacity of BMDMs and observed a significant elevation in both the stressed and basal ECAR in DAGLβ KO compared with WT counterparts ($P < 0.01$; Fig. 3 *C* and *D*). In contrast, OCR was not significantly changed in BMDMs lacking DAGLβ (*SI Appendix*, Fig. S8).

Collectively, our cell biological studies identified AMPK activation as a functional output from perturbing DAGLβ that reprograms BMDMs into a more glycolytic state. When integrated with our (chemo)proteomics data, our collective findings reveal a potential DAGLβ–LKB1–AMPK signaling axis that is important for regulating BMDM cell metabolism and signaling.

DAGLβ Inactivation Reprograms the Macrophage Phosphoproteome. To characterize cell biological alterations in DAGLβ-disrupted BMDMs, we performed quantitative phosphoproteomics analysis of SILAC BMDMs in the absence and presence of LPS stimulation. DAGLβ SILAC light (WT) and heavy (KO) BMDMs were generated and treated with LPS (100 ng/mL) to trigger the proinflammatory response as described above and in the *Materials and Methods*. Afterward, BMDMs were lysed and light and heavy proteomes combined 1:1, followed by trypsin digestion, and titanium dioxide (TiO2) enrichment of phosphopeptides (51). LC-MS/MS analysis was implemented to identify phosphopeptides and quantify changes in phosphorylation at specific protein posttranslationally modified (PTM) sites upon DAGLβ disruption (*SI Appendix*, Fig. S9). We confirmed enrichment of peptides (4,409 total phosphopeptides detected on 1,595 proteins) containing phosphorylated serines (87%), threonines (12%), and tyrosines (1%) at the expected frequency reported in literature (52, 53) (Fig. 4*A* and Dataset S1). See *SI Appendix* for details of the phosphoproteomic analyses.

Upon LPS stimulation, we identified phosphorylation events that were both up- (315) and down-regulated (529) as measured by altered phosphopeptide signals detected across 612 proteins

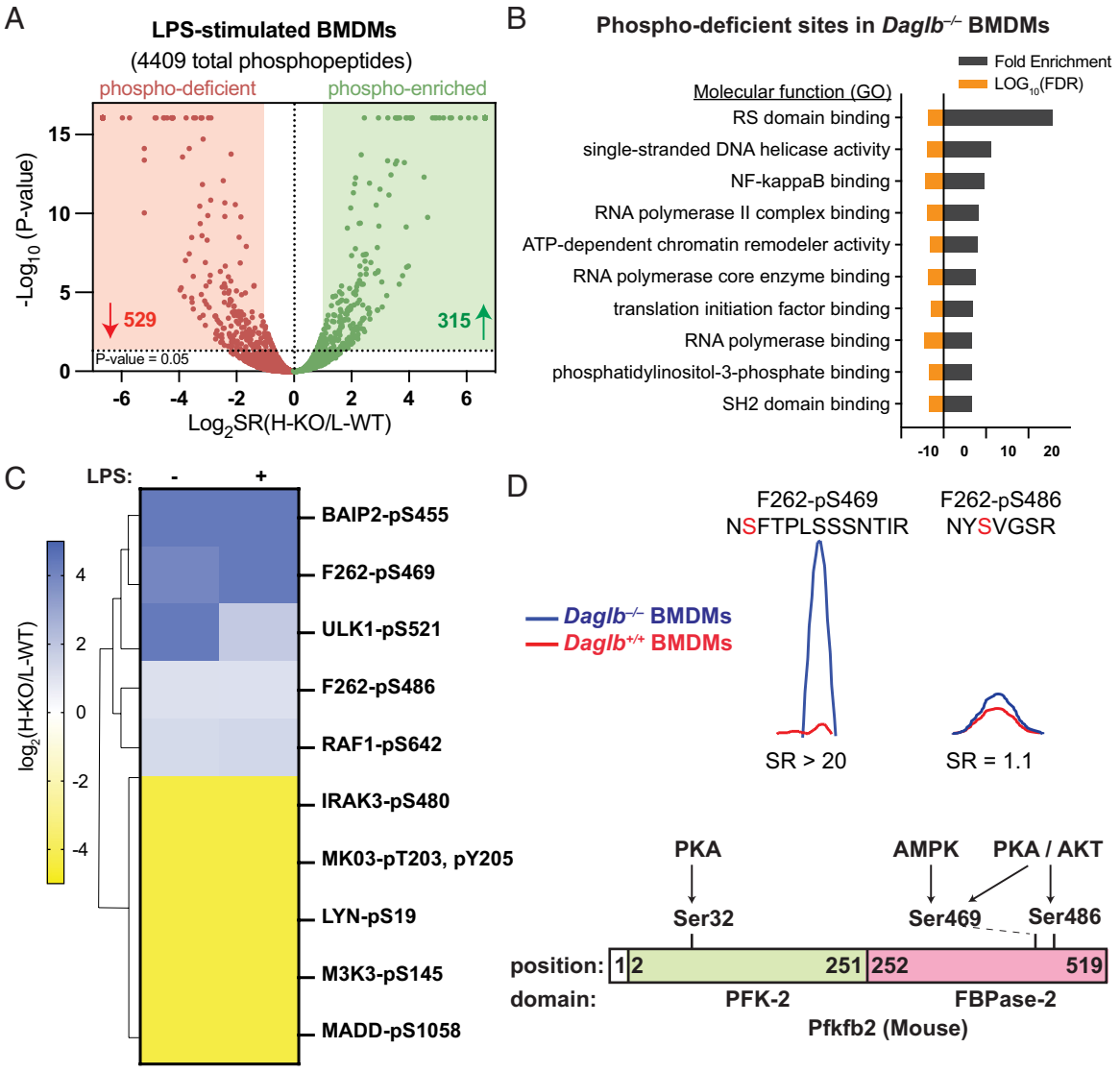

Fig. 4. DAGLβ regulation of the BMDM phosphoproteome. (*A*) Volcano plot of alterations in the phosphoproteome of DAGLβ-disrupted, LPS-stimulated BMDMs. The statistically significantly up- and down-regulated phosphosites are highlighted in green and red quadrants, respectively (*t* test, $P < 0.05$). Schematic workflow of phosphoproteomics study can be found in *SI Appendix*, Fig. S9. A heatmap of all sites quantified in basal and LPS-stimulated BMDMs can be found in *SI Appendix*, Fig. S10. (*B*) Molecular functions (PANTHER) enriched in phosphodeficient sites of LPS-stimulated, DAGLβ KO BMDMs. (*C*) Heatmap highlighting enhanced phosphorylation of the AMPK substrate PFKFB2 (F262) at S469 but not S486 in DAGLβ-disrupted BMDMs. Phosphosites displayed in the heatmap show a statistically significantly altered SR value ($P < 0.05$). (*D*) MS1 EICs of PFKFB2 phosphopeptides and reported upstream regulators of respective phosphorylation site (54). All data shown are representative of n = 3 biologically independent replicates. See Dataset S1 for complete list of SR values for phosphosites quantified.

[heavy (KO)/light (WT) SR >2 or < 0.5 and $P < 0.05$; Fig. 4*A* and Dataset S1]. Interestingly, a small fraction of phosphosites also showed comparable alterations in the absence of LPS stimulation (*SI Appendix*, Fig. S10). Down-regulated phosphosites in DAGLβ KO BMDMs were enriched for NF-κB pathway, which supports the reported antiinflammatory phenotypes from DAGLβ disruption (12–14), as well as additional functions related to transcriptional response of cells (GO analysis of phosphosites with SR < 0.5, $P < 0.05$; Fig. 4*B*).

Our phosphoproteomics investigation also provided insights into phosphorylation changes that further support activation of AMPK. Although the AMPK T172 phosphorylated site (AAPK2) was not detected, we identified increased phosphorylation of 6-phosphofructo-2-kinase/fructose-2,6-bisphosphatase 2 (PFKFB2) serine 469 (S469; S466 in human PFKFB2 or hPFKFB2), which was reported as a key site for PFKFB2 activation by AMPK (55, 56) (SR >20 in basal and LPS conditions, Fig. 4*C*). PFKFB2 controls the synthesis and degradation of fructose 2,6-bisphosphate that functions as an allosteric effector of 6-phosphofructo-1-kinase (PFK-1) to stimulate glycolysis (54). PFKFB2 activation can also be mediated by alternative kinase pathways including PKA and AKT1 that can affect phosphorylation of S469 and/or S486 (S483 in hPFKFB2) (54). We did not detect alterations in phosphorylation of PFKFB2 S486, which suggests specificity of AMPK activation in DAGLβ-disrupted BMDMs (SR ~1, Fig. 4*D*).

Further evidence for AMPK activation was provided by decreased MAPK signaling as evidenced by increased phosphorylation of an inhibitory CRAF site [RAF1 S642 (57), SR = 2.5] and decreased phosphorylation of ERK1 in DAGLβ-disrupted BMDMs (T203, Y205, SR = 0.05; Fig. 4*C*). Treatment of DAGLβ KO BMDMs with dorsomorphin resulted in significantly enhanced ERK1/2 phosphorylation at longer treatment times (*SI Appendix*, Fig. S11). Activated ERK can inhibit AMPK through phosphorylation and inactivation of LKB1 (58, 59). Comparison of phosphosites identified here with reported AMPK substrate sites revealed that many of the detected sites did not exhibit alterations like PFKFB2 S469,

suggesting that DAGLβ inactivation affected phosphorylation of a subset of AMPK substrate sites (*SI Appendix*, Fig. S12*A* and Dataset S2). We also identified AMPK substrates with alterations in phosphorylation on noncanonical sites that are candidates for future studies (ULK1-S521, LYN-S19, MADD-S1058, Fig. 4*C* and *SI Appendix*, Fig. S12*B*).

In summary, global phosphoproteomics reveal multiple lines of evidence supporting AMPK activation including phosphorylation of direct glycolytic substrates (PFKFB2) and downregulation of MAPK signaling (CRAF and ERK) that can block LKB1-AMPK signaling.

DAGLβ-AMPK Crosstalk in Pain Response In Vivo. Genetic and pharmacological inactivation of DAGLβ affects behavioral responses in preclinical models of pain (15, 60–62). DAGLβ KO mice show an antiallodynic phenotype in the LPS model of inflammatory pain, while KT109 reverses LPS-induced allodynia in WT mice (15). AMPK activation with AMP analogs (e.g., metformin, AICAR, etc.) elicits antinociception in preclinical pain assays as well as clinical pain due in part to the antiinflammatory effects of AMPK signaling (63–66). Considering our cell biological findings supporting DAGLβ-AMPK crosstalk through LKB1 activation, we tested whether AMPK signaling serves as a mechanism for mediating the antinociceptive phenotype observed in DAGLβ KO mice.

In this experiment, DAGLβ WT and KO mice were given a daily intraperitoneal (i.p.) injection of saline or dorsomorphin (20 mg kg^{-1}) for 5 d. Following the day 4 injection, each mouse was given an injection of LPS (2 μg) into the intraplantar region of the right hind paw. At 1 h after the day 5 injection, each subject was assessed for von Frey thresholds in both the LPS-treated paw and contralateral (control) paw (Fig. 5*A*). In agreement with previous findings, LPS elicited significant allodynic responses in DAGLβ WT but not in KO mice. Dorsomorphin did not affect LPS-induced allodynia in DAGLβ WT mice or affect contralateral paw thresholds in either genotype. Strikingly, this AMPK inhibitor significantly reversed the antiallodynic phenotype of DAGLβ KO mice [F(1, 20) = 57.0, $P < 0.0001$, Fig. 5*B* and *SI Appendix*, Fig. S13].

Collectively, the behavioral studies complement our cell biological findings in BMDMs to support DAGLβ-AMPK crosstalk in pain sensitization in vivo.

DAGLβ-AMPK Regulates DRG Neuron Hyperexcitability in Neuropathic Pain States. To assess further DAGLβ-AMPK signaling in nociception, we tested whether perturbing the DAGLβ-AMPK axis affects paclitaxel-induced dorsal root ganglia (DRG) neuron excitability. Macrophage infiltration and accumulation in the DRG can facilitate pronociceptive neuronal and immune cell interactions that contribute to chronic pain states (67, 68). Specifically, DRG macrophages produce inflammatory mediators that directly act on nociceptors expressing cell-surface receptors of proinflammatory signals (e.g., TNFα, prostaglandins) to alter excitability and peripheral sensitization (69). Depletion of DRG macrophages in mice prevents and reverses mechanical allodynia in neuropathic pain models (67).

Chemotherapy-induced allodynia was induced in DAGLβ WT and KO mice using a cycle of paclitaxel treatment, consisting of a single i.p. injection of paclitaxel (8 mg kg^{-1}) every other day for a total of four injections (days 1, 3, 5, and 7). To evaluate DAGLβ-AMPK crosstalk in DRG excitability, DAGLβ KO mice were given a daily i.p. injection of saline or dorsomorphin (20 mg kg^{-1}) beginning on day 8 for 6 d. Two hours after the final injection, animals were sacrificed and primary cultures of DRG neurons were prepared from adult mice as previously described (70). Whole-cell patch clamp electrophysiology measurements were performed to evaluate DRG neuron excitability as previously reported (70) and described in *SI Appendix*, *Materials and Methods*.

The threshold potential (membrane potential for the activation of an action potential) in DRG neurons from DAGLβ WT mice was significantly more negative in the paclitaxel treated compared with control mice, indicating enhanced excitability (Fig. 6*A* and Dataset S3). Compared to DRG neurons from paclitaxel-treated DAGLβ WT mice, the KO counterparts exhibited significantly reduced excitability (Fig. 6*B* and Dataset S3). Rheobase was significantly increased, and the number of evoked action potentials was reduced when compared to paclitaxel-treated DAGLβ WT DRG neurons (Fig. 6 *B* and *C*). Treatment with dorsomorphin in vivo resulted in significantly reduced rheobase and concomitant increased action potential events in DRG neurons from paclitaxel-treated DAGLβ KO mice, indicating increased neuronal excitability. No difference in neuronal excitability was observed between DAGLβ WT and dorsomorphin-treated KO DRG neurons (Fig. 6 *B* and *C* and *SI Appendix*, Fig. S14).

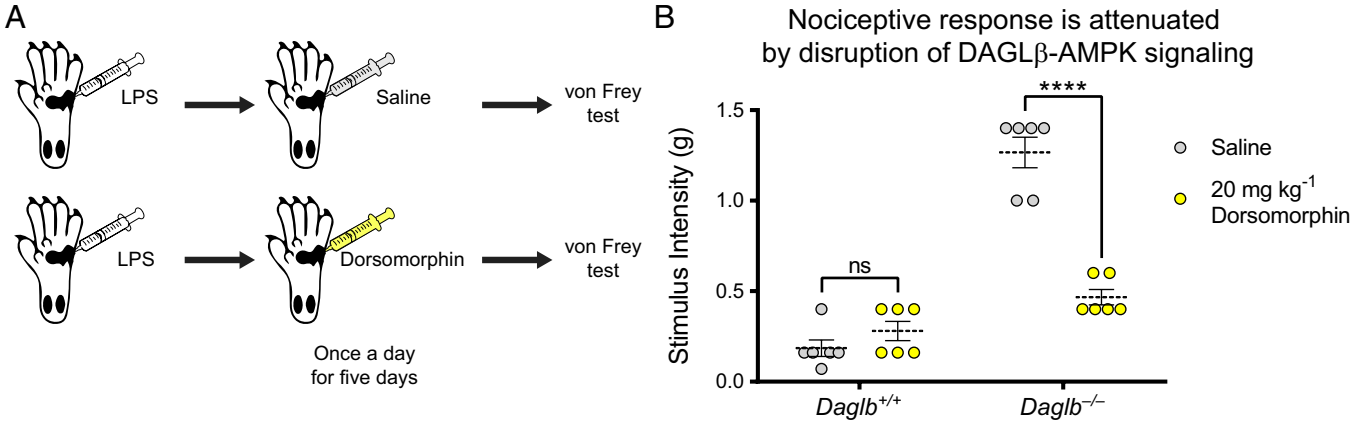

Fig. 5. DAGLβ-AMPK crosstalk in inflammatory pain response. (*A*) Schematic workflow portraying animal nociceptive behavior assessment studies. In brief, DAGLβ WT and KO mice were treated with LPS (2 μg) via intraplantar injection of the right hind paw and then treated with saline or dorsomorphin (20 mg kg^{-1}) i.p. injections daily for 5 d. (*B*) Mechanical allodynia via von Frey test was implemented to assess changes in nociceptive behavior as a result of LPS-challenge and dorsomorphin treatment. Two-way ANOVA revealed a significant genotype X dorsomorphin interaction; F(1,20) = 57.0, $P < 0.0001$. Holm-Sidak post hoc analysis; **** = $P < 0.0001$. All data shown represent mean ± SEM; (n = 6 mixed sex mice per condition). See *SI Appendix*, Fig. S13 for additional details.

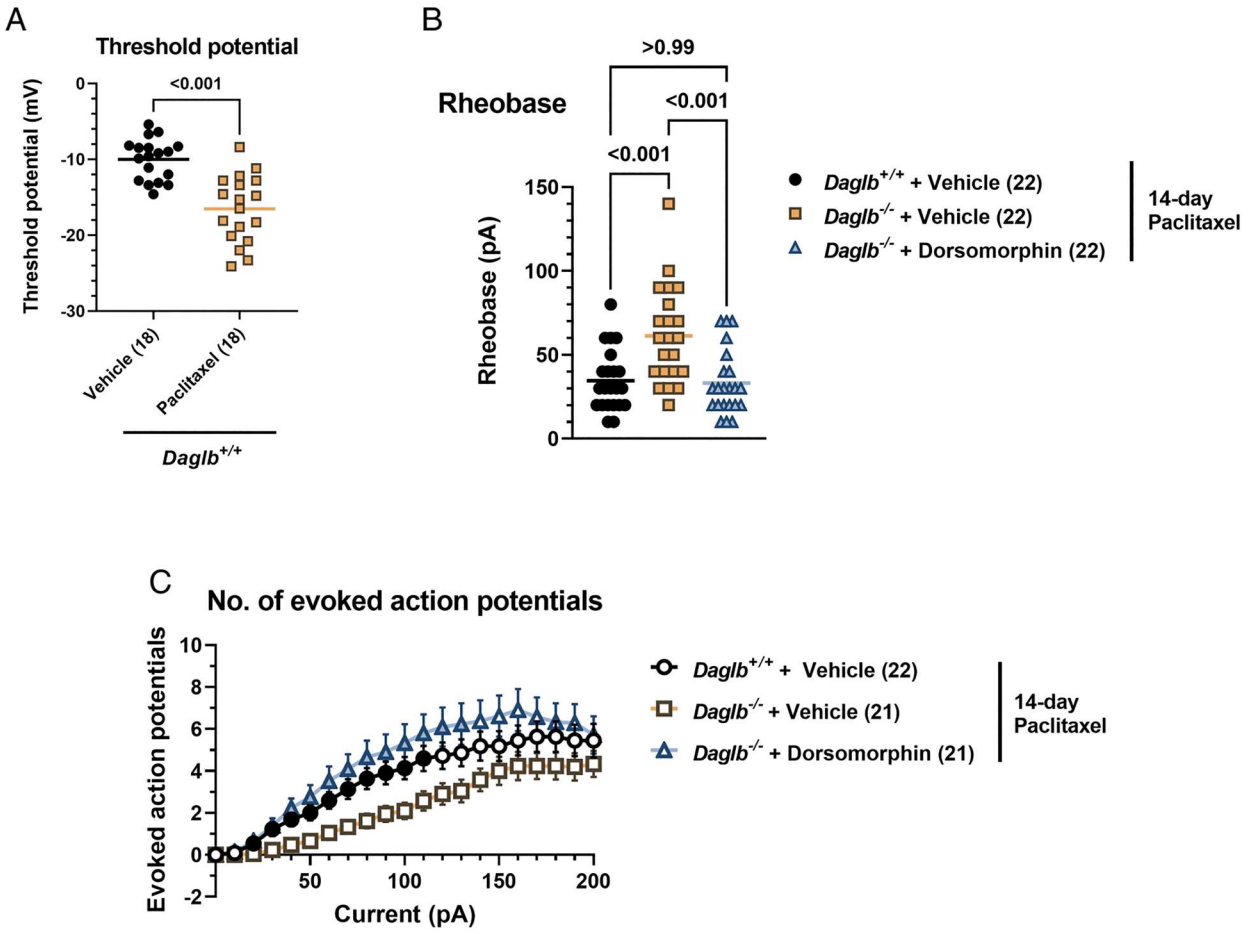

Fig. 6. Dorsomorphin induced hyperexcitability in DRG neurons from paclitaxel-treated DAGLβ KO mice. Action potential thresholds (*A*), rheobase (*B*) and current-response relationship (*C*) in small-diameter DRG neurons from DAGLβ WT or DAGLβ KO mice. Threshold potential data in (*A*) were analyzed using two-tailed unpaired Student's *t* test and rheobase data in (*B*) were analyzed using one-way ANOVA with Bonferroni's posttest. Scatter plots in (*A*) and (*B*) represent values from individual neurons and the horizontal bar indicates the mean. Number of neurons per group are indicated in the parenthesis. (*C*) Data are mean ± SEM and analyzed using two-way repeated-measures ANOVA with Bonferroni's posttest. Filled points indicate statistical significance ($P < 0.05$) versus paclitaxel + vehicle-treated DAGLβ KO neurons. Number of neurons per group are indicated in the parenthesis.

Collectively, we demonstrate that blocking AMPK through in vivo dorsomorphin treatments in DAGLβ-disrupted mice reinstated paclitaxel-induced DRG neuronal hyper-excitability. These studies provide a mechanism that accounts for the antinociceptive phenotypes resulting from disruption of DAGLβ-AMPK.

Discussion

DAGLs are enzymes that hydrolyze AA-esterified DAGs to biosynthesize 2-AG, an eicosanoid precursor, critical to inflammatory signaling (1) in microglia (13) and dendritic cells (14) and reverses nociceptive behavior in rodents (15, 60–62). Currently, DAGLβ function is ascribed principally to 2-AG-AA-eicosanoid signaling but the efficacy of DAGLβ inhibitors in inflammatory and neuropathic pain models suggests alternative pathways that are currently unknown. These studies are particularly important because long-term exposure to DAGLβ inhibitors does not produce overt metabolic, behavioral, or addictive side effects that positions this enzyme as a promising target to treat chronic pain (15). Our findings here describe a complementary kinase-mediated pathway that connects bioenergetics with endocannabinoid biosynthesis as a unique mechanism for blockade of inflammation and pain.

We deployed SILAC ABPP studies with chemical probes that profile ATP-binding pockets of kinases to identify a striking enhancement in binding activity for LKB1, the upstream regulator of AMPK (24, 34, 71, 72) in DAGLβ-disrupted BMDMs (Fig. 2). The detection of increased LKB1 binding activity in membrane but not soluble fractions of DAGLβ KO BMDMs agrees with recent reports that membrane localization, through lipid binding, of LKB1 results in activation (39). We performed orthogonal analyses to support the resulting AMPK activation through direct detection of T172 phosphorylation by western blots and global phosphoproteomics to identify increased phosphorylation on AMPK substrates at known (S469 on PFKFB2) and potentially novel sites (S521 on ULK1; Fig. 4). We interpret the negligible change in phosphorylation of PFKFB2 S486, a reported substrate site for multiple kinases including AMPK (54), as evidence for potential specificity of AMPK activation of this key glycolytic enzyme in DAGLβ-disrupted macrophages although follow-up studies are needed to provide direct verification (Fig. 4*D*). Further support was provided by chemoproteomic studies that revealed a striking increase in LKB1 binding in an otherwise unchanged kinome (Fig. 2 and *SI Appendix*, Fig. S4). These alterations in cellular signaling were complemented by increased glycolysis in DAGLβ KO BMDMs (Fig. 3 *C* and *D*).

The physiological relevance of DAGLβ-AMPK crosstalk was demonstrated in in vivo pain models that evaluated behavioral responses upon DAGLβ perturbation in the presence of the AMPK inhibitor dorsomorphin (48). Notably, dorsomorphin extinguished the antinociceptive phenotype of DAGLβ KO mice in a LPS mouse model of inflammatory pain (Fig. 5). Our electrophysiology studies in DRG neurons isolated from paclitaxel-treated DAGLβ KO mice provided mechanistic insights to DAGLβ-AMPK signaling and pain sensitization. Genetic deletion of DAGLβ reduced the characteristic hyper-excitability of DRG neurons from paclitaxel-treated mice. In support of AMPK regulation, dorsomorphin caused an emergence of paclitaxel-induced hyper-excitability in DRGs from paclitaxel-treated DAGLβ KO mice (Fig. 6).

While our studies establish DAGLβ-AMPK crosstalk in cells and in vivo, a potential role for the DAGLα isoform in regulating bioenergetic pathways, to the best of our knowledge, remains unknown. Future studies aimed at understanding regulation of bioenergetics by DAGL isoforms may provide insight into developing targeted agents for tissue- and cell type–specific AMPK activation. Our mechanistic understanding of DAGLβ-AMPK crosstalk in pain would be further advanced by identifying the cell type(s) mediating DRG neuron hyper-excitability. Given that DAGLβ shows minimal expression and activity in neurons (13), a potential explanation is that DRG macrophages (67, 68) mediate the in vivo change in sensory neuron hyperresponsiveness. As LKB1-selective inhibitors become available, their evaluation in future studies using chemoproteomics and complementary activity assays (39) will be important to test further whether LKB1 serves as the principal AMPK-activating kinase in DAGLβ-disrupted systems. Orthogonal methods for evaluating AMPK activity are also needed given that ATP acyl phosphate probe binding to the catalytic subunit of AMPK was unchanged in our chemoproteomic studies and likely explained by the complicated activation mechanism involving sensing and binding of AMP, ADP, and ATP by this kinase (20).

In conclusion, our findings establish a critical link between endocannabinoid biosynthesis and macrophage bioenergetics in pathogenic pain response. The cellular and in vivo findings support disruption of DAGLβ as a unique approach for activating AMPK signal transduction for developing nonopioid analgesics. Identifying alternative pathways for AMPK activation and regulation is not only important for understanding fundamental cell metabolism but also has direct and broader impacts on human health. It is estimated that greater than 150 million people worldwide take the AMPK activator drug metformin (73). Metformin is associated with a variety of side effects, including birth defects in cases where the father used this drug for treatment of diabetes (74). Thus, developing more targeted AMPK activators represents a need of clinical interest.

Materials and Methods

Details on SILAC bone marrow derived macrophage (BMDM) differentiation, gel-based competitive activity-based protein profiling (ABPP), quantitative LC-MS/MS proteomics, chemoproteomics and phosphoproteomics, extracellular flux analysis, behavioral assessment of animal nociception, and electrophysiology of dorsal root ganglia (DRG) neurons can be found in *SI Appendix*.

Data, Materials, and Software Availability. Proteomics data have been deposited at ProteomeXchange via the PRIDE database (http://www.proteomexchange.org) and are publicly available under accession numbers PXD047413 and https://doi.org/10.6019/PXD047413 (75). RNA-seq data are available on NCBI Gene Expression Omnibus, under accession number GSE249312 (76).

ACKNOWLEDGMENTS. We thank all members of the Hsu Lab for helpful discussions and review of the manuscript. This work was supported by the NIH Grants [DA053107 to T.B.W.; P30DA033934 (H.I.A. and A.H.L.); F31DK108553 (V.S.); T32GM007055 (V.S. and C.M.U.), P01HL120840 (N.L.), DA043571 and GM144472 to K.-L.H.], American Heart Association (15 PRE 255600036 to V.S.), Mini-fellowship from the Society for Redox Biology and Medicine (V.S.), VCU School of Pharmacy Start-up funds (A.H.L.), University of Virginia Cancer Center (NCI Cancer Center Support Grant No. 5P30CA044579-27 to K.-L.H.), NSF (CHE-1942467 to K.-L.H.), the Robbins Family MRA Young Investigator Award from the Melanoma Research Alliance (http://doi.org/10.48050/pc.gr.80540 to K.-L.H.), the Owens Family Foundation (K.-L.H.), and the Mark Foundation for Cancer Research (Emerging Leader Award to K.-L.H.).

Author affiliations: [a]Department of Chemistry, University of Virginia, Charlottesville, VA 22904; [b]Department of Pharmacology and Toxicology, Virginia Commonwealth University, Richmond, VA 23298; [c]Department of Pharmacology, University of Virginia School of Medicine, Charlottesville, VA 22908; [d]Department of Medicinal Chemistry, Virginia Commonwealth University, Richmond, VA 23298; [e]Department of Molecular Physiology and Biological Physics, University of Virginia, Charlottesville, VA 22908; and [f]University of Virginia Cancer Center, Cancer Biology Program, University of Virginia, Charlottesville, VA 22903

1. T. Bisogno *et al.*, Cloning of the first sn1-DAG lipases points to the spatial and temporal regulation of endocannabinoid signaling in the brain. *J. Cell Biol.* **163**, 463–468 (2003).
2. Y. Gao *et al.*, Loss of retrograde endocannabinoid signaling and reduced adult neurogenesis in diacylglycerol lipase knock-out mice. *J. Neurosci.* **30**, 2017–2024 (2010).
3. A. Tanimura *et al.*, The endocannabinoid 2-arachidonoylglycerol produced by diacylglycerol lipase alpha mediates retrograde suppression of synaptic transmission. *Neuron* **65**, 320–327 (2010).
4. T. R. Baffi, A. C. Newton, Protein kinase C: Release from quarantine by mTORC2. *Trends Biochem. Sci.* **47**, 518–530 (2022).
5. V. E. Marquez, P. M. Blumberg, Synthetic diacylglycerols (DAG) and DAG-lactones as activators of protein kinase C (PK-C). *Acc Chem. Res.* **36**, 434–443 (2003).
6. D. Ogasawara *et al.*, Rapid and profound rewiring of brain lipid signaling networks by acute diacylglycerol lipase inhibition. *Proc. Natl. Acad. Sci. U.S.A.* **113**, 26–33 (2016).
7. B. C. Shonesy *et al.*, Genetic disruption of 2-arachidonoylglycerol synthesis reveals a key role for endocannabinoid signaling in anxiety modulation. *Cell Rep.* **9**, 1644–1653 (2014).
8. S. Yoon, K. Myczek, P. Penzes, cAMP signaling-mediated phosphorylation of diacylglycerol lipase alpha regulates interaction with Ankyrin-G and dendritic spine morphology. *Biol. Psychiatry* **90**, 263–274 (2021).
9. W. Fyke, J. M. Alarcon, M. Velinov, K. K. Chadman, Pharmacological inhibition of the primary endocannabinoid producing enzyme, DGL-alpha, induces autism spectrum disorder-like and co-morbid phenotypes in adult C57BL/J mice. *Autism Res.* **14**, 1375–1389 (2021).
10. L. D. Schurman *et al.*, Diacylglycerol lipase-alpha regulates hippocampal-dependent learning and memory processes in mice. *J. Neurosci.* **39**, 5949–5965 (2019).
11. V. S. Cavener *et al.*, Inhibition of diacylglycerol lipase impairs fear extinction in mice. *Front Neurosci.* **12**, 479 (2018).
12. K. L. Hsu *et al.*, DAGLbeta inhibition perturbs a lipid network involved in macrophage inflammatory responses. *Nat. Chem. Biol.* **8**, 999–1007 (2012).
13. A. Viader *et al.*, A chemical proteomic atlas of brain serine hydrolases identifies cell type-specific pathways regulating neuroinflammation. *eLife* **5**, e12345 (2016).
14. M. Shin, A. Buckner, J. Prince, T. N. J. Bullock, K. L. Hsu, Diacylglycerol lipase-beta is required for TNF-alpha response but not CD8(+) T cell priming capacity of dendritic cells. *Cell Chem. Biol.* **26**, 1036–1041.e3 (2019).
15. J. L. Wilkerson *et al.*, Diacylglycerol lipase beta inhibition reverses nociceptive behaviour in mouse models of inflammatory and neuropathic pain. *Br J. Pharmacol.* **173**, 1678–1692 (2016).
16. M. Schafers, M. Marziniak, L. S. Sorkin, T. L. Yaksh, C. Sommer, Cyclooxygenase inhibition in nerve-injury- and TNF-induced hyperalgesia in the rat. *Exp. Neurol.* **185**, 160–168 (2004).
17. D. C. Broom *et al.*, Cyclooxygenase 2 expression in the spared nerve injury model of neuropathic pain. *Neuroscience* **124**, 891–900 (2004).
18. T. S. King-Himmelreich *et al.*, AMPK contributes to aerobic exercise-induced antinociception downstream of endocannabinoids. *Neuropharmacology* **124**, 134–142 (2017).
19. T. S. King-Himmelreich *et al.*, AMP-activated kinase and the endogenous endocannabinoid system might contribute to antinociceptive effects of prolonged moderate caloric restriction in mice. *Mol. Pain* **13**, 1744806917703111 (2017).
20. A. Gonzalez, M. N. Hall, S. C. Lin, D. G. Hardie, AMPK and TOR: The Yin and Yang of cellular nutrient sensing and growth control. *Cell Metab.* **31**, 472–492 (2020).
21. S. Herzig, R. J. Shaw, AMPK: Guardian of metabolism and mitochondrial homeostasis. *Nat. Rev. Mol. Cell Biol.* **19**, 121–135 (2018).
22. B. Xiao *et al.*, Structural basis for AMP binding to mammalian AMP-activated protein kinase. *Nature* **449**, 496–500 (2007).
23. G. J. Gowans, S. A. Hawley, F. A. Ross, D. G. Hardie, AMP is a true physiological regulator of AMP-activated protein kinase by both allosteric activation and enhancing net phosphorylation. *Cell Metab* **18**, 556–566 (2013).
24. S. A. Hawley *et al.*, Complexes between the LKB1 tumor suppressor, STRAD alpha/beta and MO25 alpha/beta are upstream kinases in the AMP-activated protein kinase cascade. *J. Biol.* **2**, 28 (2003).

25. S. P. Davies, N. R. Helps, P. T. Cohen, D. G. Hardie, 5′-AMP inhibits dephosphorylation, as well as promoting phosphorylation, of the AMP-activated protein kinase. Studies using bacterially expressed human protein phosphatase-2C alpha and native bovine protein phosphatase-2AC. *FEBS Lett.* **377**, 421–425 (1995).
26. M. Suter *et al.*, Dissecting the role of 5′-AMP for allosteric stimulation, activation, and deactivation of AMP-activated protein kinase. *J. Biol. Chem.* **281**, 32207–32216 (2006).
27. G. Rena, D. G. Hardie, E. R. Pearson, The mechanisms of action of metformin. *Diabetologia* **60**, 1577–1585 (2017).
28. L. A. O'Neill, D. G. Hardie, Metabolism of inflammation limited by AMPK and pseudo-starvation. *Nature* **493**, 346–355 (2013).
29. B. Kola *et al.*, Cannabinoids and ghrelin have both central and peripheral metabolic and cardiac effects via AMP-activated protein kinase. *J. Biol. Chem.* **280**, 25196–25201 (2005).
30. B. Kola *et al.*, The CB1 receptor mediates the peripheral effects of ghrelin on AMPK activity but not on growth hormone release. *FASEB J.* **27**, 5112–5121 (2013).
31. Y. Lu, B. C. Akinwumi, Z. Shao, H. D. Anderson, Ligand activation of cannabinoid receptors attenuates hypertrophy of neonatal rat cardiomyocytes. *J. Cardiovasc. Pharmacol.* **64**, 420–430 (2014).
32. L. J. Sun *et al.*, Endocannabinoid system activation contributes to glucose metabolism disorders of hepatocytes and promotes hepatitis C virus replication. *Int. J. Infect Dis.* **23**, 75–81 (2014).
33. E. R. Hudson *et al.*, A novel domain in AMP-activated protein kinase causes glycogen storage bodies similar to those seen in hereditary cardiac arrhythmias. *Curr. Biol.* **13**, 861–866 (2003).
34. A. Woods *et al.*, LKB1 is the upstream kinase in the AMP-activated protein kinase cascade. *Curr. Biol.* **13**, 2004–2008 (2003).
35. S. A. Hawley *et al.*, Calmodulin-dependent protein kinase kinase-beta is an alternative upstream kinase for AMP-activated protein kinase. *Cell Metab.* **2**, 9–19 (2005).
36. A. Woods *et al.*, Ca2+/calmodulin-dependent protein kinase kinase-beta acts upstream of AMP-activated protein kinase in mammalian cells. *Cell Metab.* **2**, 21–33 (2005).
37. A. Hemminki *et al.*, A serine/threonine kinase gene defective in Peutz-Jeghers syndrome. *Nature* **391**, 184–187 (1998).
38. D. B. Shackelford, R. J. Shaw, The LKB1-AMPK pathway: Metabolism and growth control in tumour suppression. *Nat. Rev. Cancer* **9**, 563–575 (2009).
39. G. Dogliotti *et al.*, Membrane-binding and activation of LKB1 by phosphatidic acid is essential for development and tumour suppression. *Nat. Commun.* **8**, 15747 (2017).
40. M. Shin, T. B. Ware, K. L. Hsu, DAGL-beta functions as a PUFA-specific triacylglycerol lipase in macrophages. *Cell. Chem. Biol.* **27**, 314–321.e5 (2020).
41. R. L. McCloud *et al.*, Deconstructing lipid kinase inhibitors by chemical proteomics. *Biochemistry* **57**, 231–236 (2018).
42. M. P. Patricelli *et al.*, In situ kinase profiling reveals functionally relevant properties of native kinases. *Chem. Biol.* **18**, 699–710 (2011).
43. M. P. Patricelli *et al.*, Functional interrogation of the kinome using nucleotide acyl phosphates. *Biochemistry* **46**, 350–358 (2007).
44. E. Zeqiraj, B. M. Filippi, M. Deak, D. R. Alessi, D. M. van Aalten, Structure of the LKB1-STRAD-MO25 complex reveals an allosteric mechanism of kinase activation. *Science* **326**, 1707–1711 (2009).
45. N. Kannan, A. F. Neuwald, Did protein kinase regulatory mechanisms evolve through elaboration of a simple structural component? *J. Mol. Biol.* **351**, 956–972 (2005).
46. L. Zhang *et al.*, Functional role of histidine in the conserved His-x-Asp motif in the catalytic core of protein kinases. *Sci. Rep.* **5**, 10115 (2015).
47. L. Kullmann, M. P. Krahn, Controlling the master-upstream regulation of the tumor suppressor LKB1. *Oncogene* **37**, 3045–3057 (2018).
48. G. Zhou *et al.*, Role of AMP-activated protein kinase in mechanism of metformin action. *J. Clin. Invest.* **108**, 1167–1174 (2001).
49. N. Handa *et al.*, Structural basis for compound C inhibition of the human AMP-activated protein kinase alpha2 subunit kinase domain. *Acta Crystallogr. D Biol. Crystallogr.* **67**, 480–487 (2011).
50. V. Serbulea *et al.*, Macrophage phenotype and bioenergetics are controlled by oxidized phospholipids identified in lean and obese adipose tissue. *Proc. Natl. Acad. Sci. U.S.A.* **115**, E6254–E6263 (2018).
51. J. Villen, S. P. Gygi, The SCX/IMAC enrichment approach for global phosphorylation analysis by mass spectrometry. *Nat. Protoc* **3**, 1630–1638 (2008).
52. S. J. Humphrey *et al.*, Dynamic adipocyte phosphoproteome reveals that Akt directly regulates mTORC2. *Cell Metab.* **17**, 1009–1020 (2013).
53. A. Lundby *et al.*, Quantitative maps of protein phosphorylation sites across 14 different rat organs and tissues. *Nat. Commun.* **3**, 876 (2012).
54. M. H. Rider *et al.*, 6-phosphofructo-2-kinase/fructose-2,6-bisphosphatase: Head-to-head with a bifunctional enzyme that controls glycolysis. *Biochem. J.* **381**, 561–579 (2004).
55. A. S. Marsin *et al.*, Phosphorylation and activation of heart PFK-2 by AMPK has a role in the stimulation of glycolysis during ischaemia. *Curr. Biol.* **10**, 1247–1255 (2000).
56. A. S. Marsin, C. Bouzin, L. Bertrand, L. Hue, The stimulation of glycolysis by hypoxia in activated monocytes is mediated by AMP-activated protein kinase and inducible 6-phosphofructo-2-kinase. *J. Biol. Chem.* **277**, 30778–30783 (2002).
57. M. K. Dougherty *et al.*, Regulation of Raf-1 by direct feedback phosphorylation. *Mol. Cell* **17**, 215–224 (2005).
58. S. Papa, P. M. Choy, C. Bubici, The ERK and JNK pathways in the regulation of metabolic reprogramming. *Oncogene* **38**, 2223–2240 (2019).
59. J. Yuan, X. Dong, J. Yap, J. Hu, The MAPK and AMPK signalings: Interplay and implication in targeted cancer therapy. *J. Hematol. Oncol.* **13**, 113 (2020).
60. M. Shin *et al.*, Liposomal delivery of diacylglycerol lipase-beta inhibitors to macrophages dramatically enhances selectivity and efficacy in vivo. *Mol. Pharm.* **15**, 721–728 (2018).
61. J. L. Wilkerson *et al.*, Investigation of diacylglycerol lipase alpha inhibition in the mouse lipopolysaccharide inflammatory pain model. *J. Pharmacol. Exp. Ther.* **363**, 394–401 (2017).
62. I. A. Khasabova *et al.*, Inhibition of DAGLbeta as a therapeutic target for pain in sickle cell disease. *Haematologica* **108**, 859–869 (2023).
63. Q. L. Mao-Ying *et al.*, The anti-diabetic drug metformin protects against chemotherapy-induced peripheral neuropathy in a mouse model. *PLoS One* **9**, e100701 (2014).
64. T. J. Price, V. Das, G. Dussor, Adenosine monophosphate-activated protein kinase (AMPK) activators for the prevention, treatment and potential reversal of pathological pain. *Curr. Drug Targets* **17**, 908–920 (2016).
65. O. Q. Russe *et al.*, Activation of the AMP-activated protein kinase reduces inflammatory nociception. *J. Pain* **14**, 1330–1340 (2013).
66. K. E. Inyang *et al.*, Alleviation of paclitaxel-induced mechanical hypersensitivity and hyperalgesic priming with AMPK activators in male and female mice. *Neurobiol. Pain* **6**, 100037 (2019).
67. X. Yu *et al.*, Dorsal root ganglion macrophages contribute to both the initiation and persistence of neuropathic pain. *Nat. Commun.* **11**, 264 (2020).
68. H. Zhang *et al.*, Dorsal root ganglion infiltration by macrophages contributes to paclitaxel chemotherapy-induced peripheral neuropathy. *J. Pain* **17**, 775–786 (2016).
69. A. I. Basbaum, D. M. Bautista, G. Scherrer, D. Julius, Cellular and molecular mechanisms of pain. *Cell* **139**, 267–284 (2009).
70. G. R. Ross, A. R. Gade, W. L. Dewey, H. I. Akbarali, Opioid-induced hypernociception is associated with hyperexcitability and altered tetrodotoxin-resistant Na+ channel function of dorsal root ganglia *Am. J. Physiol. Cell Physiol.* **302**, C1152–C1161 (2012).
71. S. P. Hong, F. C. Leiper, A. Woods, D. Carling, M. Carlson, Activation of yeast Snf1 and mammalian AMP-activated protein kinase by upstream kinases. *Proc. Natl. Acad. Sci. U.S.A.* **100**, 8839–8843 (2003).
72. R. J. Shaw *et al.*, The tumor suppressor LKB1 kinase directly activates AMP-activated kinase and regulates apoptosis in response to energy stress. *Proc. Natl. Acad. Sci. U.S.A.* **101**, 3329–3335 (2004).
73. H. An, L. He, Current understanding of metformin effect on the control of hyperglycemia in diabetes. *J. Endocrinol.* **228**, R97–R106 (2016).
74. M. J. Wensink *et al.*, Preconception antidiabetic drugs in men and birth defects in offspring: A nationwide cohort study. *Ann. Intern Med.* **175**, 665–673 (2022).
75. M. Chen *et al.*, Endocannabinoid biosynthetic enzymes regulate pain response via LKB1–AMPK signaling proteomics data. ProteomeXchange. https://doi.org/10.6019/PXD047413. Deposited 30 November 2023.
76. M. Chen *et al.*, Endocannabinoid biosynthetic enzymes regulate pain response via LKB1–AMPK signaling gene expression data. NCBI Gene Expression Omnibus (GEO). https://www.ncbi.nlm.nih.gov/geo/query/acc.cgi?acc=GSE249312. Deposited 4 December 2023.